

Performance Analysis of 6G Communication Links in the Presence of Phase Noise

Arianna Halamandaris

Department of Electrical and
Computer Engineering

California State University Northridge, USA
Email: arianna.halamandaris.552@my.csun.edu

Md Sahabul Alam

Department of Electrical and
Computer Engineering

California State University Northridge

Imtiaz Ahmed

Department of Electrical Engineering
Howard University, USA

Email: imtiaz.ahmed@howard.edu

Kamrul Hasan

Department of Electrical Engineering
Tennessee State University, USA
Email: mhasan1@tnstate.edu

Georges Kaddoum

Department of Electrical Engineering
ETS, Montreal, Canada
Email: georges.kaddoum@etsmtl.ca

Abstract—As the infrastructure of fifth generation (5G) is integrated worldwide, sixth generation (6G) of cellular communications standard is being developed as the next generation of high-speed wireless communications and internet connectivity. The goal of most innovations in communications is higher data rates and reduced latency. Thus, 6G is envisioned to operate on terahertz (THz) frequencies to leverage wide bandwidth of spectrum. Hardware operating at such high frequencies will be more susceptible to phase noise, or jitter in the time domain, because every time the frequency of the clock is upconverted, the phase noise increases. In addition, 6G will use higher-order modulation schemes to transmit data at higher speeds. It is unknown what modulations 6G communication systems will use, but 5G uses up to 256 QAM when connections are strong, thus we can assume 6G will possibly go even higher than that. Higher data rates require higher signal-to-noise ratios to reduce the bit error rate. Thus the higher the modulation order, the greater the impact of phase noise. The purpose of this paper is to further understand how 6G communication links will be impacted by phase noise. Simulation results demonstrate that there is a significant performance degradation due to phase noise when moving from 5G (Sub-6 GHz and millimeter Wave) to possible 6G carrier frequency ranges and adopting higher order modulation techniques.

Index Terms—5G/6G, Phase noise, QAM

I. INTRODUCTION

There is always a growing need for higher data rates and channel capacity in digital communications. This was certainly the case in the transition from fourth generation (4G) to fifth generation (5G), with an increasing desire for media streaming, virtual reality, and all at extremely high speeds. The bandwidth and data rate demands keep increasing over the years, considering the future of augmented reality and messaging via holographic communications create a need for much higher capability than what 5G offers at present. To meet the needs of the ever-growing demand for greater data throughput, sixth generation (6G) digital communication networks are going to be developed over the course of the next decade [1]–[3].

As the 6G communications technology is further planned and developed, new challenges arise [2], [3]. To increase data rates and network capacities, 6G is aiming to operate in the Sub-terahertz (Sub-THz) frequency range, namely 95–300 GHz [4]. Working at these frequencies introduces a host of challenges [5] [6]. For instance, the challenge of operating at high frequencies at reasonable distances and the large-scale adoption of 6G despite its limited range of operation necessitates the development of complex network architectures, which will likely necessitate artificial intelligence (AI) driven design and development [3]. Moreover, designing antennas, amplifiers, and other hardware to operate at THz bands presents many challenges. Opening the radio frequencies (RF) spectrum to the sub-THz range will push the limits of semiconductor design, antenna design, and clock design. To start, the antennas are much smaller, and present a challenge when considering designing a compact system with limited interference and coupling. In addition, building and packaging efficient semiconductors at such high frequencies and with such high bandwidths is a challenge in and of itself. Amplifier design, both low-noise and power amplifiers present their own challenges. Considering the many channels that are implemented to a massive multi-input multi-output (MIMO) system, which will be critical for the operation of 6G networks, phase noise (PN) is even more pronounced due to the need to synchronize the many carriers. A comparison of the various frequency bands that are used in previous generations of cellular networks, as well as that of 6G is represented in Fig. 1. Notice how the frequencies being explored for 6G are significantly higher than that of any other previous generation of digital communications.

The main focus of this paper is the challenges that arise when designing hardware to work at such high frequencies, specifically the challenge of PN that arises from using local oscillators to upconvert these frequencies and ultimately how this noise effects system performance. Considering that

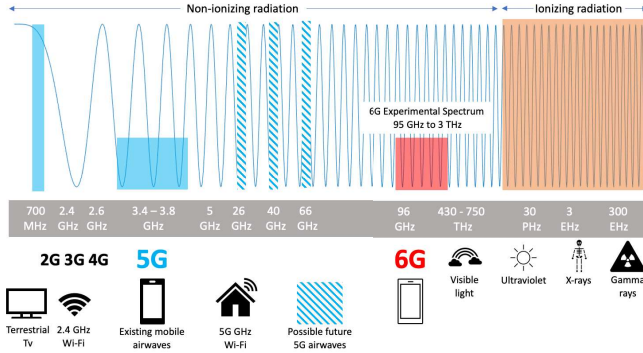


Fig. 1. Electromagnetic spectrum allocation for different application scenarios.

modern communications rely on digital modulation schemes, up and down conversion is critical to system operations. Namely, data processing at intermediate frequencies (IF) and baseband is significantly easier than processing at RF. In fact, in digital communications, processing must be done at baseband, thus the higher the frequency operation, the greater the frequency conversion must be.

PN has been a focus of research in the past decade due to the great effects in the communications and radar space. The desire to use higher frequencies for communications increases this research interest even more due to the known degradations that high levels of PN causes, particularly at high frequencies. Being able to characterize the system level effects and model PN realistically can improve system design by informing design choices. Ultimately, understanding the behavior of PN and its effects on a communications system could reducing the amount of symbol errors caused by PN by adopting the hardware design, the design of the modulation scheme or digital compensation for this issue [7], [8].

Recently, several studies have been conducted in mitigating PN by leveraging AI tools to alleviate the run-time computational complexity of conventional schemes. In [9], a deep learning (DL) based low-complexity algorithm is proposed for compensating the effects of PN in channel estimation and data detection for multicarrier systems by substituting the iterative processes of the conventional estimators. A data-driven joint channel, PN, and in-phase and quadrature-phase (IQ) imbalance estimation scheme has been proposed in [10] for multi-carrier MIMO full-duplex communication systems. A similar contribution has been made in [11] for generalized frequency division multiplexing (GFDM) communication systems. Phase noise compensation by exploiting the coherence bandwidth of millimeter-wave channels has been introduced and thoroughly analyzed in [12]. As PN is considered an integral part of developing 6G communication systems operating in THz bands, creating an efficient, insightful, and mathematically tractable model of PN is essential. Following this essence, in [7], an appropriate choice of a phase noise model for Sub-THz communications has been discussed, and two efficient models have been

proposed, evaluated, and analyzed. Moreover, a time-series model has been developed for phase noise in [8] to provide insights into the performance of a THz-band communication system. The performance of THz-band transmission in intelligent reflecting surface (IRS)-aided communication systems has been investigated under the combined effects of channel fading, THz pointing error (TPE), and statistical PN due to imperfect phase compensation in [13]. In [14], an analysis has been done on the collective impact of channel aging and PN for IRS-aided systems. Phase calibration for IRS-assisted millimeter wave communication systems has been developed in [15]. In [16], an improved mixed phased/retrodirective array has been developed for the unmanned aerial vehicle (UAV)-assisted communication network operated on the THz band. An achievable throughput is calculated for UAV communications supported by IRS in [17] while considering the impact of PN. Motivated by these recent interests on PN, in this paper, we consider the impact of PN on the performance of higher order modulation techniques that are assumed to be used in 6G networks using Sub-THz frequency bands.

The rest of the paper is organized as follows. In Section II, we introduce phase noise, modeling of phase noise, and its specifications for 5G. Modulation techniques for 5G and 6G and the impact of phase noise on these modulation techniques is detailed in Section III. We show the simulation results in Section IV. Section V presents the paper's conclusion.

II. PHASE NOISE

Although this paper specifically explores the impacts of PN when present in a local oscillator, PN also effects many other parts of a communications system. Namely, impacting MIMO systems, network timing, higher order modulations, and millimeter wave (mmWave) components, all which are critical to link performance. A communication link needs to be synchronous in order to demodulate a signal, for example, in a higher order quadrature amplitude modulation (QAM) technique, amplitude and phase of the signal is what determines its value. Thus, if there is PN present in the transmitted signal, there will be phase errors when demodulating. This process will be described in much greater detail later in this paper.

PN is presented in a communications link when upconverting from intermediate frequencies up to the desired output, which in the 6G case will likely be from 95 GHz up to 300 GHz. In order to do this, there is a local oscillator clock which is mixed with the signal excision at IF. Mixing two signals generates a carrier frequency, which is equal to the sum of the carrier frequencies of the added signals. Typically, the local oscillators used in these scenarios are designed to have extremely low PN. These oscillators are typically designed to operate between 100 MHz to 500 MHz [18], and are sometimes paired with a phase locked loop (PLL) in order to keep PN at a minimum value and reduce phase errors. Even though the PN levels of these stable clocks are very low, when they are used for up conversion, the resulting PN of the mixed signal goes up 6 dB for each frequency

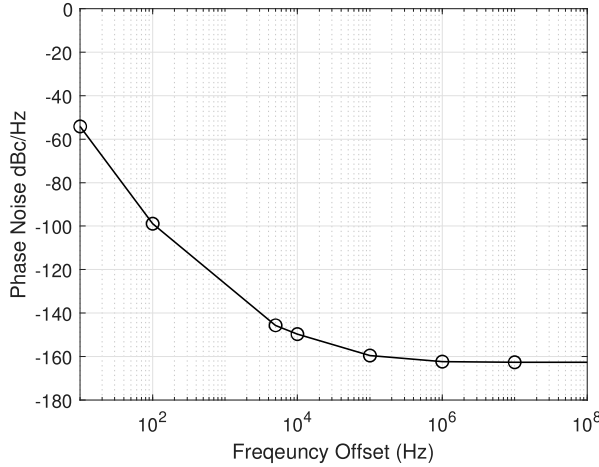


Fig. 2. Representation of phase noise of 500 MHz 5G base station oscillator.

doubling. In the case of 6G, the frequency is being mixed up as much as 3000 times. The resulting PN is expressed as [19]

$$\Delta L(f) = 20 \log_{10} N, \quad (1)$$

where N is the multiple which the frequency is increased. For example, PN of a 500 MHz clock upconverted to 300 GHz results in a 55 dB increase in PN.

A. Modeling of Phase Noise

To evaluate a communication link operation in the presence of PN, it is imperative to understand how PN usually appears in an oscillator. Phase noise is typically modeled using Leeson's equation as follows [19]

$$L = 10 \log \left[\frac{2F_k T}{P_{sig}} \left\{ 1 + \left(\frac{w_0}{2Q\Delta w} \right)^2 \right\} \left(1 + \frac{w_1}{\Delta w} \right) \right]. \quad (2)$$

Here, F_k is an empirically determined curve fitting variable, P_{sig} is the power of the transmitted signal, w_0 is the oscillation frequency of the clock signal, w_1 is the corner frequency determining where the $1/f$ noise will flatten out, and finally Q is the oscillator quality factor. Leeson's equation generates a PN mask that looks much like that in Fig. 2.

B. Phase Noise Specification for 5G

Exploiting (2) and given an example oscillator that meets specification to be used in a 5G base station, we have generated a model of PN that we will consider to represent PN in a 6G system. The PN mask in Fig. 2 is the specification for a 500 MHz clock. Considering the effect of frequency on PN in (2), a higher frequency clock would be preferred. For example, a 500 MHz clock would be preferable over a 100 MHz clock. In Fig. 2, the Y-axis unit is dBc/Hz, which represents how much power in the log scale (decibels) down from the power at the carrier frequency the signal is as a function of the offset frequency in Hertz (Hz). As the signal gets further from the carrier, it is expected to emit less power.

Transistors are known to produce $1/f$ noise, which states that the noise decreases as a function of the frequency. In Fig. 2, this behavior is represented as the straight line from 10 Hz to 10 kHz. As was previously described in (2), the corner frequency determines where the flat, or 'white' noise begins. In the 5G base station oscillator, white noise occurs at around 100 kHz.

In all simulations described in this paper, the PN mask model presented in Fig. 2 is used; however, depending on the desired carrier frequency of the transmitted signal, this will be scaled up or down by (1).

III. MODULATION SCHEMES FOR 5G AND 6G

5G communication system is currently employed to use 16, 64, and 256 QAM depending on the signal-to-noise ratio (SNR) in the environment that it is broadcasting. The idea behind QAM is that information can be transmitted by distinguishing the amplitude from symbol to symbol, as well as the phase (quadrature). QAM is a popular modulation technique because it has the combined benefits of both phase shift keying and amplitude shift keying and can transmit more information without sacrificing risk of error, power or bandwidth compared to other techniques.

If the communications system is working in an environment with significant amounts of environmental noise and the received signal is not significantly higher than the noise floor, then the 5G system preferably use a 16 QAM constellation scheme in order to transmit symbols. This is due to the fact that higher order modulations are much more susceptible to noise. This idea is shown when observing Figs. 3, 4, and 5. In these figures, the constellation diagrams showing the received symbols in reference to the transmit symbols where the transmit symbols are represented by a red crosshair, and the received symbols are represented by yellow dots. In Figs. 3, 4, and 5, X-axis and Y-axis represent the in-phase and quadrature amplitude of the signal, respectively. In Fig. 3, a 16 QAM modulation scheme is shown transmitting through a channel impaired by Additive White Gaussian Noise (AWGN) as well as low levels of PN.

When compared to the constellation diagram in Fig. 4, the symbols in Fig. 3 are significantly more distinct and easier to distinguish. This is due to the fact that the PN in Fig. 4 is 20 dBc/Hz higher than that of Fig. 3. Although they are using the same constellation, the data transmitted for the latter case will have a smaller chance of being successfully demodulated. This phenomenon becomes significantly worse at higher modulation orders. From analyzing these constellation diagrams, it is clear how PN translates into errors in a QAM modulation. PN results in errors in phase, thus creating a trail of received constellations surrounding the transmitted symbol, which vary in angle.

In Fig. 5, a 256 QAM is transmitted over a channel with AWGN and higher PN implemented. It is clear to visualize how higher orders of QAM are more susceptible to PN due to the distance between symbols being much shorter than a lower order modulation scheme. Typically, the receiver

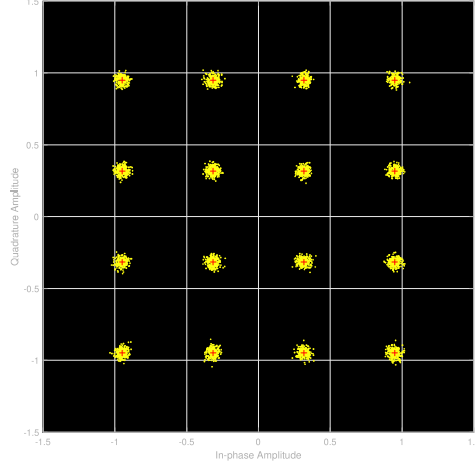


Fig. 3. Constellation diagram of 16 QAM with -91 dBc/Hz phase Noise.

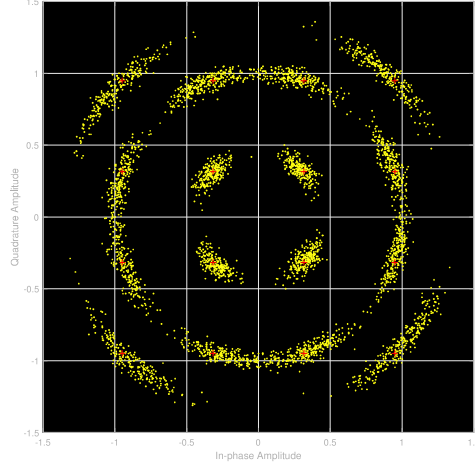


Fig. 4. Constellation diagram of 16 QAM with -71 dBc/Hz phase Noise.

demodulates QAM by thresholding between symbols, thus the closer the symbols are, the more likely there are to be errors due to phase and amplitude noise. Note that the symbols further from the center are much less susceptible to PN than those further out from the center.

The modulation schemes that will be used in the next generation of communications are still unknown. Considering the use of QAM in 4G and 5G, and the increase in modulation order with each generation, in this paper the assumption is that 6G will not only use QAM, but will employ higher order QAM modulations than its' predecessor.

IV. SIMULATION RESULTS

The simulation results shown in this paper to represent the impact of PN on the higher order modulations that are assumed to be used in 6G networks, as well as Sub-THz

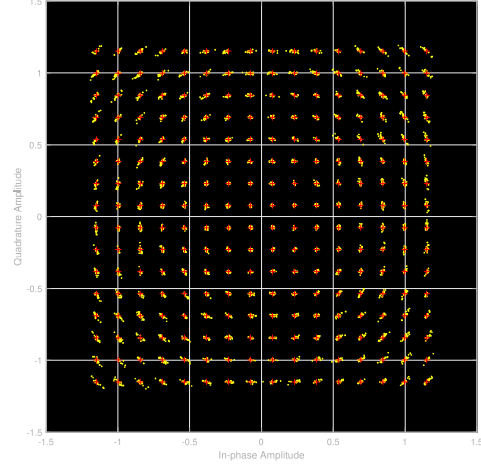


Fig. 5. Constellation diagram of 256 QAM with -71 dBc/Hz phase Noise.

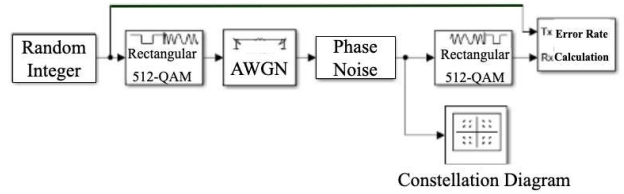


Fig. 6. Simulink model of communication links.

communications are generated using Simulink in conjunction with a MATLAB script.

A. Simulink Communications Link Model

The block diagram of the model used for all simulations is displayed in Fig. 6. This model first generates M random integers, where M is the modulation order defined in the rectangular QAM modulation and demodulation block. The sample rate of the generated symbols must also be defined and be consistent throughout the simulation. In order to determine symbol error rate (SER) or bit error rate (BER), a MATLAB script is implemented to increase the SNR in the AWGN block after each run and collect the error rate that is determined in the final block. The constellation diagrams displayed in Figs. 3, 4, and 5 are all generated using this model.

The PN specification displayed in Fig. 2 has been implemented in the phase noise block of the diagram. This phase noise block takes power and frequency offset values to generate a filter that resembles the PN plot in Fig. 2. This is a well-known method of modeling PN in simulations. In Fig. 2, the PN is modeled from 10 Hz to 100 MHz. For

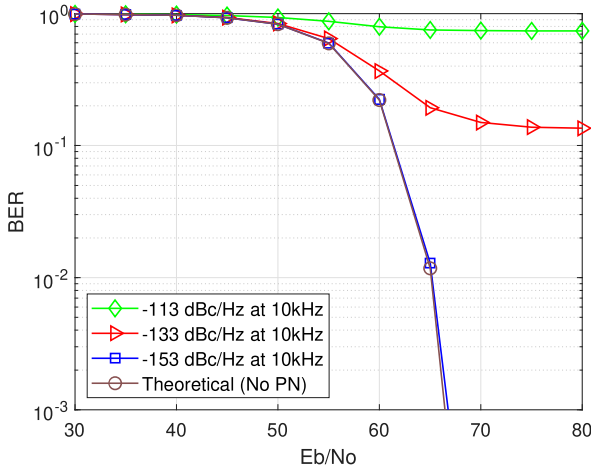


Fig. 7. BER performance of 256 QAM modulation scheme in the presence of phase noise at the carrier frequency of 24 GHz.

the purpose of this paper, we limited the generated PN of the system to 10 kHz. This is consistent with the $1/f$ noise component that was discussed earlier in this paper.

B. Phase Noise Model for 5G and 6G

As mentioned earlier, all of the following simulations are performed by scaling the PN specification of a 5G base station local oscillator using (1). The resulting PN at 10 kHz is displayed in Table I that is calculated by adding (1) to the PN mask in Fig. 2 up to 10 kHz.

TABLE I
PHASE NOISE SPECIFICATION (USED IN THE MODEL)

Carrier Frequency	Phase Noise at 10kHz offset
24 GHz	-113 dBc/Hz
100GHz	-100 dBc/Hz
300 GHz	-91 dBc/Hz

C. Results for 5G

It is expected that when modulating over 5G bands, e.g., around 20 GHz to 44 GHz, the system should perform relatively well. The results of this simulation, using 256 QAM at 24 GHz, is displayed in Fig. 7. The theoretical performance is also displayed, that is the performance of the system by increasing bit energy with an AWGN distribution having no PN is implemented. By observation, the simulation using the PN from Fig. 2 in a 5G system performs nearly identically to the theoretical performance at 40 dBc/Hz below the PN at 24 GHz. An important thing to note for this simulation, as well as all simulations to follow, is that these results are obtained while considering only PN in the system. No other noise is considered. Thus a real system may perform much worse than this result, but the goal of this paper is to determine the results considering only PN effects.

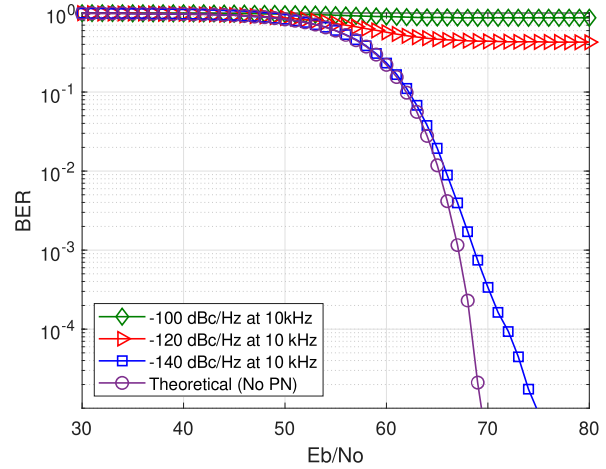


Fig. 8. BER performance of 256 QAM modulation scheme in the presence of phase noise at the carrier frequency of 100 GHz.

D. Results for 6G

In this section, the frequencies tested are at the low (100 GHz) and high (300 GHz) end of the Sub-THz range. The actual frequencies which will be used in 6G is still an area of further research and exploration. Furthermore, the clock being used is assumed to be similar to that in the 5G system, being merely increased in power as obtained from (1). The PN values at 10 kHz is provided in Table I. Thus, for a communications link operating at 24 GHz, the PN level at 10 kHz is -113 dBc/Hz, and the theoretical PN mask for a 6G system operating at 100 GHz and 300 GHz is -100 dBc/Hz and -91 dBc/Hz, respectively. As discussed earlier, it is expected that the PN levels will be higher when the system is operating at higher frequencies.

Based on the assumption that 6G may use higher order QAM modulations than a 5G system to transmit and receive data, the simulations were performed for 256 QAM, 512 QAM, and 1024 QAM. Based on communication theory and PN effects previously discussed in this paper, it is expected that the performance of the communication link is worse when considering PN effects and operating at higher frequencies. In other words, the PN will have more of an effect when the source of the noise, the oscillator, is being used to upconvert the signal to higher frequencies for transmission. This finding can be seen when comparing the results of equivalent QAM orders (i.e. 256 QAM) with different modulating frequencies (100 GHz and 300 GHz) as shown in Figs. 8 and 9, respectively. One can observe that the PN level for the 100 GHz carrier frequency is lower than that operating at 300 GHz, thus the performance is notably better when comparing the results at a theoretical 40 dB improvement in PN.

It is also expected that PN will have a greater effect when using higher modulation orders. This is illustrated in Fig. 10 when comparing 256 QAM, 512 QAM, and

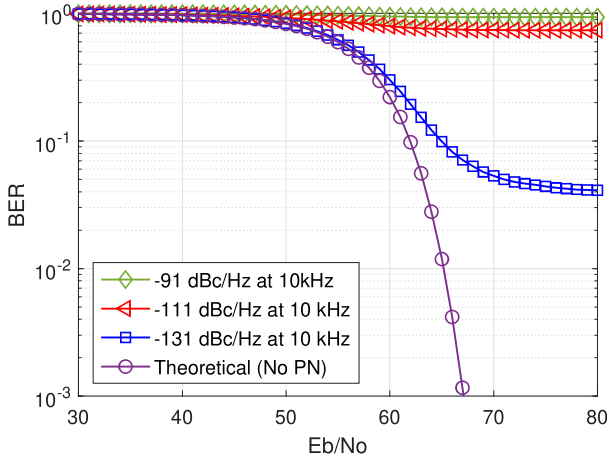


Fig. 9. BER performance of 256 QAM modulation scheme in the presence of phase noise at the carrier frequency of 300 GHz.

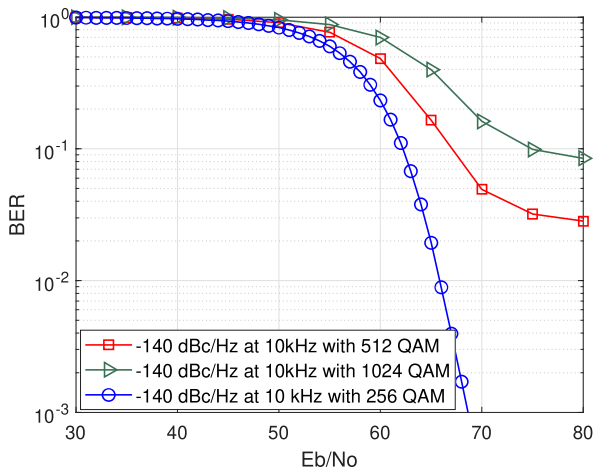


Fig. 10. BER performance of different QAM modulation schemes in the presence of phase noise at the carrier frequency of 100 GHz.

1024 QAM operating at similar carrier frequencies. From Fig. 10, it is evident that there is a significant performance degradation when higher order modulation techniques are used considering the same carrier frequency.

V. CONCLUSION

In this paper, the impact of PN on the performance of higher order modulations that are assumed to be used in 6G networks, as well as Sub-THz communications are analyzed and presented. Considering all of the assumptions that were necessary to make in order to obtain the simulation results provided above, it was shown that the error performance of a 6G communication link will be more degraded compared to 5G in the presence of PN. Assuming that PN is a key performance indicator for 6G communications, these results suggest the need for an improvement in clock performance

during the continuous movement towards communication links operating at higher data rates.

In a nutshell, these observations and findings must be revisited and adapted as 6G standards and classification processes are developed and design decisions are finalized.

REFERENCES

- [1] P. Yang, Y. Xiao, M. Xiao, and S. Li, "6G wireless communications: Vision and potential techniques," *IEEE network*, vol. 33, no. 4, pp. 70–75, 2019.
- [2] H. Tataria, M. Shafi, M. Dohler, and S. Sun, "Six critical challenges for 6G wireless systems: A summary and some solutions," *IEEE Vehicular Technology Magazine*, vol. 17, no. 1, pp. 16–26, 2022.
- [3] M. Z. Chowdhury, M. Shahjalal, S. Ahmed, and Y. M. Jang, "6G wireless communication systems: Applications, requirements, technologies, challenges, and research directions," *IEEE Open Journal of the Communications Society*, vol. 1, pp. 957–975, 2020.
- [4] W. Jiang and H. D. Schotten, "The kick-off of 6G research worldwide: An overview," in *2021 7th International Conference on Computer and Communications (ICCC)*. IEEE, 2021, pp. 2274–2279.
- [5] C. De Lima, D. Belot, R. Berkvens, A. Bourdoux, D. Dardari, M. Guillaud, M. Isomursu, E.-S. Lohan, Y. Miao, A. N. Barreto *et al.*, "Convergent communication, sensing and localization in 6G systems: An overview of technologies, opportunities and challenges," *IEEE Access*, vol. 9, pp. 26 902–26 925, 2021.
- [6] I. F. Akyildiz, J. M. Jornet, and C. Han, "Terahertz band: Next frontier for wireless communications," *Physical communication*, vol. 12, pp. 16–32, 2014.
- [7] S. Bicais and J.-B. Dore, "Phase noise model selection for sub-THz communications," in *2019 IEEE Global Communications Conference (GLOBECOM)*. IEEE, 2019, pp. 1–6.
- [8] J. Cheah, "Phase noise time series model," in *MILCOM 2021 - 2021 IEEE Military Communications Conference (MILCOM)*, 2021, pp. 139–144.
- [9] A. Mohammadian, C. Tellambura, and G. Y. Li, "Deep learning-based phase noise compensation in multicarrier systems," *IEEE Wireless Communications Letters*, vol. 10, no. 10, pp. 2110–2114, 2021.
- [10] —, "Deep learning LMMSE joint channel, PN, and IQ imbalance estimator for multicarrier MIMO full-duplex systems," *IEEE Wireless Communications Letters*, vol. 11, no. 1, pp. 111–115, 2021.
- [11] A. Mohammadian and C. Tellambura, "Joint channel and phase noise estimation and data detection for GFDM," *IEEE Open Journal of the Communications Society*, vol. 2, pp. 915–933, 2021.
- [12] M. Chung, L. Liu, and O. Edfors, "Phase-noise compensation for OFDM systems exploiting coherence bandwidth: Modeling, algorithms, and analysis," *IEEE Transactions on Wireless Communications*, vol. 21, no. 5, pp. 3040–3056, 2021.
- [13] O. R. Durgada, V. K. Chapala, and S. Zafaruddin, "RIS-THz wireless communication with random phase noise and misaligned transceiver," *arXiv preprint arXiv:2211.08690*, 2022.
- [14] W. Jiang and H. D. Schotten, "Performance impact of channel aging and phase noise on intelligent reflecting surface," *IEEE Communications Letters*, 2022.
- [15] J. Zhang, X. Hu, and C. Zhong, "Phase calibration for intelligent reflecting surfaces assisted millimeter wave communications," *IEEE Transactions on Signal Processing*, vol. 70, pp. 1026–1040, 2022.
- [16] A. Salman, S. Almekdad, and M. Alhariri, "Improvement of phase noise performance in tracking array of UAV signal based on mixed phased/retrodirective array," *Progress In Electromagnetics Research C*, vol. 95, pp. 195–207, 2019.
- [17] M. Al-Jarrah, E. Alsusa, A. Al-Dweik, and D. K. So, "Capacity analysis of IRS-based UAV communications with imperfect phase compensation," *IEEE Wireless Communications Letters*, vol. 10, no. 7, pp. 1479–1483, 2021.
- [18] Seiko Epson Corporation, "Performance requirements for reference clocks for 5G communications," Suwa, Nagano, Japan, Tech. Rep. OUT-20-5536, Accessed on May 8, 2022.
- [19] T. H. Lee and A. Hajimiri, "Oscillator phase noise: A tutorial," *IEEE journal of solid-state circuits*, vol. 35, no. 3, pp. 326–336, 2000.